DALTON

The reactivity of [2.2.2]paracyclophane towards $Cr(CO)_6$: experimental and theoretical considerations

Paul J. Dyson,*[,a] **David G. Humphrey,**[b] **John E. McGrady,**[c] **Priya Suman**[a] **and Derek Tocher**[b]

[a] *Department of Chemistry, Imperial College of Science, Technology and Medicine,*
South Kensington, London SW7 2AY, UK
[b] *Christopher Ingold Laboratories, University College London, 20 Gordon Street,*
London WC1H 0AJ, UK
[c] *Department of Chemistry, The Australian National University, Canberra, ACT 0200, Australia*

The reactivity of [2.2.2]paracyclophane ($C_{24}H_{24}$) towards hexacarbonylchromium has been examined and the rates of reaction for the formation of mono-, bis- and tris-complexes established. The structures of $[Cr(CO)_3(\eta\text{-}C_{24}H_{24})]$ and $[\{Cr(CO)_3\}_2(\eta\text{-}C_{24}H_{24})]$ have been established by single crystal X-ray diffraction. These experimental observations have been interpreted using approximate density functional molecular orbital calculations.

The synthesis and characterisation of cyclophane–metal complexes has attracted a great deal of attention, and this area has recently been reviewed.[1] Interest in these complexes has been stimulated by the unique properties which cyclophanes add to the area of transition metal–arene chemistry and the ultimate goal in this area is to prepare a polymeric material comprising alternating cyclophane–metal units which may have interesting electrical and magnetic properties.[2]

Unlike other planar polyarenes, the π electron density on the rings of cyclophanes overlap so that a through-space electron-transfer mechanism is a dominant factor in influencing their chemistry.[3] This is exemplified by reactivity studies with the transition metals. For example, the crystal structure of the [2.2]paracyclophane complex, $[Cr(CO)_3(\eta\text{-}C_{16}H_{16})]$, reveals that the two arene rings move closer together upon complexation to the electron-withdrawing $Cr(CO)_3$ group.[4] It was also found that the second ring is deactivated towards further substitution and more aggressive conditions are required to form the bis(tricarbonylchromium) complex.[5]

We recently compared the reactivity of [2.2]paracyclophane with the non-strained arene, *p*-xylene.[6] The presence of two arenes rings lying parallel to each other at a distance considerably less than a typical van der Waals contact confers increased reactivity to [2.2]paracyclophane due to the π–π repulsions between the arene rings, which increase electron density on the outer faces of the ligand, thereby increasing its nucleophilicity relative to *p*-xylene. The thermodynamic stability of [2.2]paracyclophane complexes is also larger than expected and arises from the reduction in these π–π repulsions in the coordinated complex, a consequence of the electron withdrawing nature of metal fragments. As a continuation of these studies we have conducted some related experiments on [2.2.2]paracyclophane which are described in this paper.

Results and Discussion

Arene–tricarbonylchromium complexes, *i.e.* $[Cr(CO)_3(\eta\text{-arene})]$, are conveniently prepared in high yield from the direct reaction of $[Cr(CO)_6]$ and the appropriate arene in high boiling ethers, typically 1,4-dioxane.[7] It is generally accepted that the substitution mechanism is first order with the rate determining step involving dissociation of the three carbonyl ligands.[8,9] The mono-, bis- and tris-tricarbonylchromium complexes of [2.2.2]paracyclophane, $[Cr(CO)_3(\eta\text{-}C_{24}H_{24})]$ **1**, $[\{Cr(CO)_3\}_2(\eta\text{-}C_{24}H_{24})]$ **2** and $[\{Cr(CO)_3\}_3(\eta\text{-}C_{24}H_{24})]$ **3**, have previously been prepared and characterised.[10] We have, however, determined the rate of formation for the sequential addition of $\{Cr(CO)_3\}$ to [2.2.2]paracyclophane, *viz*. **1**–**3** by monitoring the disappearance of $[Cr(CO)_6]$ [ν(CO) 1980 cm^{-1}] with time (see Experimental section for details). The rate constants for the complexations were estimated at 1.75×10^{-6}, 0.88×10^{-6} and 0.80×10^{-6} s^{-1} for the first, second and third complexation reactions, respectively. It is noteworthy that there is a large difference in the rate of reaction between the first complexation and the other two, and that the difference in rates between the second and third complexations is quite small. These effects are rationalised using density functional molecular orbital calculations (see below) using structural parameters obtained from the molecular structures of compounds **1** and **2**.

Structural characterisation of compounds 1 and 2

Single crystals of compound **1** were obtained from a solution of dichloromethane–hexane stored at 4 °C for 24 h while compound **2** was crystallised from dichloromethane–hexane by slow evaporation. The molecular structures of **1** and **2** are shown in Figs. 1 and 2, respectively, and relevant bond parameters are listed in Tables 1 and 2. The molecular structures of compounds **1** and **2** are closely related and will be discussed together. They differ in that in **2**, two $\{Cr(CO)_3\}$ units are coordinated to the ligand as opposed to only one in the other complex. The chromium–ring carbon bond distances indicate that the ring is not totally planar as the distances involving the bridgehead carbon atoms are slightly longer than the remaining

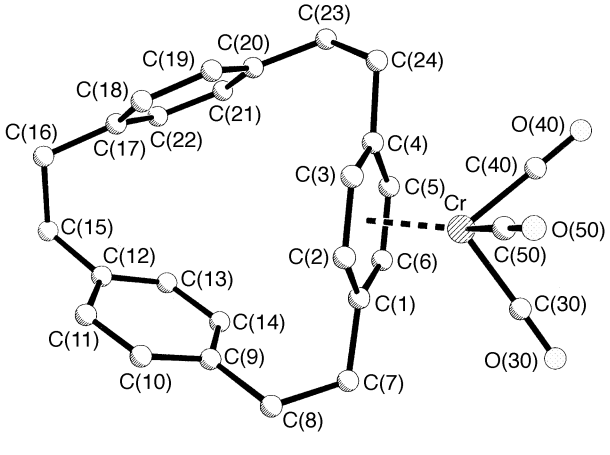

Fig. 1 Molecular structure of $[Cr(CO)_3(\eta\text{-}C_{24}H_{24})]$ **1** in the solid state

Table 1 Bond lengths (Å) for compound **1**

Cr–C, ring		Ring 3, C–C	
Cr–C(1)	2.288(5)	C(17)–C(18)	1.380(7)
Cr–C(2)	2.252(6)	C(17)–C(22)	1.377(7)
Cr–C(3)	2.250(5)	C(18)–C(19)	1.392(8)
Cr–C(4)	2.301(5)	C(19)–C(20)	1.382(7)
Cr–C(5)	2.240(5)	C(20)–C(21)	1.385(7)
Cr–C(6)	2.248(5)	C(21)–C(22)	1.373(7)
Ring 1, C–C		Aliphatic links, C–C	
C(1)–C(2)	1.400(7)	C(1)–C(7)	1.501(7)
C(1)–C(6)	1.414(7)	C(7)–C(8)	1.50(1)
C(2)–C(3)	1.407(7)	C(8)–C(9)	1.515(8)
C(3)–C(4)	1.383(7)	C(12)–C(15)	1.506(8)
C(4)–C(5)	1.412(7)	C(15)–C(16)	1.537(8)
C(5)–C(6)	1.398(8)	C(16)–C(17)	1.506(8)
Ring 2, C–C		C(20)–C(23)	1.490(7)
C(9)–C(10)	1.375(9)	C(23)–C(24)	1.548(7)
C(9)–C(14)	1.377(8)	C(4)–C(24)	1.505(7)
C(10)–C(11)	1.368(8)	Carbonyls	
C(11)–C(12)	1.389(7)	Cr–C(30)	1.851(6)
C(12)–C(13)	1.380(8)	C(30)–O(30)	1.142(8)
C(13)–C(14)	1.386(8)	Cr–C(40)	1.836(6)
		C(40)–O(40)	1.149(8)
		Cr–C(50)	1.839(5)
		C(50)–O(50)	1.159(6)

Table 2 Bond lengths (Å) for compound **2**

Cr–C, ring		Ring 3, C–C	
Cr(1)–C(11)	2.251(8)	C(27)–C(28)	1.390(14)
Cr(1)–C(12)	2.209(9)	C(27)–C(32)	1.386(14)
Cr(1)–C(13)	2.215(8)	C(28)–C(29)	1.40(2)
Cr(1)–C(14)	2.234(8)	C(29)–C(30)	1.381(4)
Cr(1)–C(15)	2.231(8)	C(30)–C(31)	1.408(14)
Cr(1)–C(16)	2.195(8)	C(31)–C(32)	1.38(2)
Cr(2)–C(19)	2.231(8)	Aliphatic links, C–C	
Cr(2)–C(20)	2.223(8)	C(11)–C(34)	1.516(12)
Cr(2)–C(21)	2.204(8)	C(14)–C(17)	1.511(12)
Cr(2)–C(22)	2.230(9)	C(17)–C(18)	1.532(14)
Cr(2)–C(23)	2.195(9)	C(18)–C(19)	1.510(11)
Cr(2)–C(24)	2.221(9)	C(22)–C(25)	1.498(12)
Ring 1, C–C		C(25)–C(26)	1.55(2)
C(11)–C(12)	1.404(12)	C(26)–C(27)	1.520(14)
C(11)–C(16)	1.395(12)	C(30)–C(33)	1.503(14)
C(12)–C(13)	1.438(12)	C(33)–C(34)	1.528(14)
C(13)–C(14)	1.385(12)	Carbonyls	
C(14)–C(15)	1.398(13)	Cr(1)–C(1)	1.833(10)
C(15)–C(16)	1.433(12)	O(1)–C(1)	1.154(11)
Ring 2, C–C		Cr(1)–C(2)	1.835(10)
C(19)–C(20)	1.419(12)	O(2)–C(2)	1.149(12)
C(19)–C(24)	1.382(13)	Cr(1)–C(3)	1.846(11)
C(20)–C(21)	1.380(12)	O(3)–C(3)	1.153(12)
C(21)–C(22)	1.418(13)	Cr(2)–C(4)	1.838(10)
C(22)–C(23)	1.403(13)	O(4)–C(4)	1.143(11)
C(23)–C(24)	1.418(13)	Cr(2)–C(5)	1.821(11)
		O(5)–C(5)	1.154(13)
		Cr(2)–C(6)	1.837(11)
		O(6)–C(6)	1.157(13)

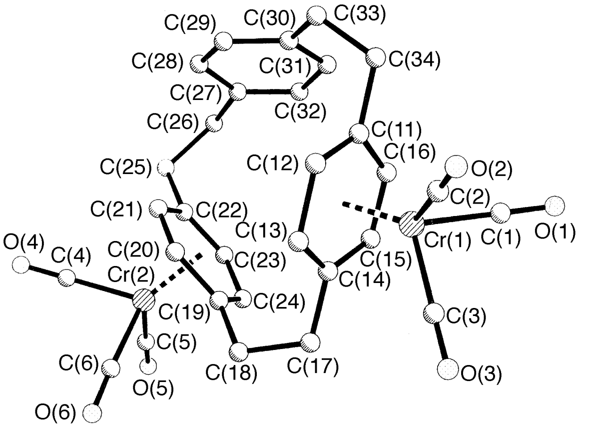

Fig. 2 Molecular structure of $[\{Cr(CO)_3\}_2(\eta\text{-}C_{24}H_{24})]$ **2** in the solid state

four C–C bonds. The Cr–C (ring) distances average 2.29 and 2.24 Å in **1** and 2.24 and 2.21 Å for **2** with respect to the bridgehead and C–H carbon atoms, respectively. It is clear that the difference between these parameters in **2** are less than in **1** (Δ 0.05 in **1** and Δ 0.03 in **2**, although this is near the limit of meaningful significance for **2**). This indicates that as the number of electron withdrawing $\{Cr(CO)_3\}$ units increases the intramolecular repulsion between the rings decreases. This is in keeping with both the kinetic data and the results obtained from density functional molecular orbital calculations (see below). The dihedral angle formed between the 'boat ends' of the co-ordinated rings is 4.9° in **1** and 1.1 and 1.2° in **2**. The corresponding dihedral angles for the unco-ordinated rings are 4.1 and 2.9° in **1** and 6.6° in **2**. These values indicate that two $\{Cr(CO)_3\}$ fragments are required in order for significant distortions of the [2.2.2]paracyclophane to take place. The average C–C distances of co-ordinated rings are longer than the unco-ordinated rings [mean 1.40 *versus* 1.38 Å in **1** and 1.41 and 1.40 *versus* 1.39 Å in **2**]. Again, this is in keeping with the decrease in bond order associated with co-ordination of the $\{Cr(CO)_3\}$ units. The orientations of the tricarbonyl units with respect to the underlying C_6 ring also differ. In **1** the carbonyls adopt a staggered conformation with respect to the C atoms of the ring while in **2** they more closely approach an eclipsed conformation. However, the barrier to rotation in arene–tricarbonylchromium complexes is typically very low, and as such variations of the orientation of the carbonyls with respect to the C_6 ring are commonly encountered.

While the idealised [2.2.2]paracyclophane molecule can be imagined to have the centroids of the rings at the vertices of an equilateral triangle with the rings perpendicular to it (D_{3h} symmetry), the planes of the three rings in **1** do not all point towards each other. This is quite unusual as the rings in [2.2.2]paracyclophane itself and **2** align so as to face the centre of the molecule. However, in **1** one of the rings is twisted by *ca.* 27° from the parallel with respect to the mean planes of the other rings. It is not fully understood why this is the case but it is probably due to intermolecular forces rather than intramolecular ones.

Density functional molecular orbital calculations

In our previous paper[6] we examined the origin of the enhanced nucleophilicity of [2.2]paracyclophane relative to *p*-xylene, and also the greater thermodynamic stability of the complex $[Cr(CO)_3(\eta\text{-}C_{16}H_{16})]$, relative to $[Cr(CO)_3(\eta\text{-}C_6H_4Me_2\text{-}1,4)]$. Both phenomena were traced to the destabilising influence of the repulsions between the occupied π orbitals on the benzene ring (transforming as a_{1g} and e_{1u} in D_{6h} symmetry). The π electron density is forced out of the transannular region, thereby making it more available to an approaching electrophile, increasing the rate of reaction. The electron-withdrawing metal fragment then reduces the π density at the co-ordinated ring, thereby reducing the π–π repulsions in $[Cr(CO)_3(\eta\text{-}C_{16}H_{16})]$, stabilising it relative to other simple monoarene complexes. In this paper we extend the analysis given in ref. 6 to include the successive addition of two or more $\{Cr(CO)_3\}$ fragments to both [2.2]- and [2.2.2]-paracyclophane.

Throughout this work similar assumptions to those in the previous paper are made. Firstly, it is assumed that cyclophanes can be adequately modelled by simply placing idealised benzene rings at the appropriate points in space (*i.e.* it is assumed that

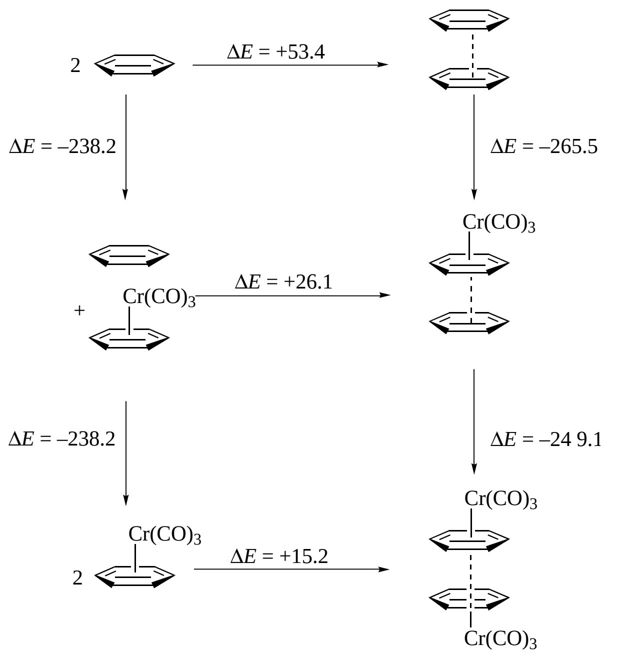

Scheme 1 The thermodynamic cycle relating successive association energies of $\{Cr(CO)_3\}$ (kJ mol^{-1}) to changes in π–π repulsion energies for the model system for [2.2]paracyclophane

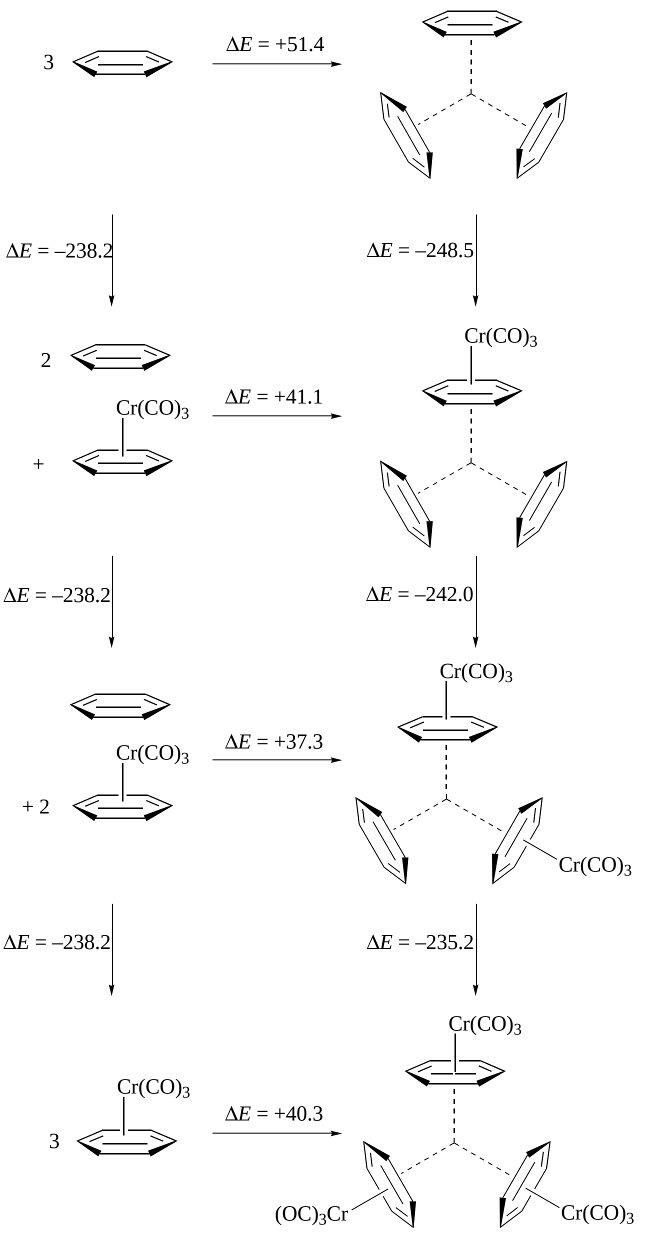

Scheme 2 The thermodynamic cycle relating successive association energies of $\{Cr(CO)_3\}$ (kJ mol^{-1}) to changes in π–π repulsion energies for the model system for [2.2.2]paracyclophane

the through-space π–π interactions are the dominant pathway for electronic communication). This assumption is least valid for [2.2]paracyclophane where there is a distinct distortion of the arene rings towards a bowl-shaped geometry, but even in this case the assumption of planar benzene rings reproduced the correct trends in reactivity and stability. Secondly, it is assumed that the dominant conformation in solution corresponds to the case where the faces of all the arene rings point inwards towards the centre of the molecule. The other computational details remain exactly as before. Thermodynamic cycles are constructed from successive metallation of [2.2]- and [2.2.2]-paracyclophane, relating successive association energies to differences in π–π repulsions in the various species.†

The data summarised in Scheme 1 confirm that the association of $\{Cr(CO)_3\}$ with [2.2]paracyclophane is some 27 kJ mol^{-1} more favourable than with benzene, due to the reduction in π–π repulsions by the tricarbonylchromium group. The addition of a second $\{Cr(CO)_3\}$ unit further reduces the repulsion between the arene rings, but this time only by 11 kJ mol^{-1}, and so the complexation of the second $\{Cr(CO)_3\}$ fragment is still favoured over that of benzene, but by less than half as much as the first. Once again the thermodynamically favourable association can be linked to the enhanced rate of reaction by noting that the residual π–π repulsions in $[Cr(CO)_3(\eta\text{-}C_{16}H_{16})]$ will result in greater electron density on the outer face of the unco-ordinated ring, and hence to greater nucleophilicity. Therefore, on the basis of energetic arguments alone, we would anticipate the rate for the reaction of $[Cr(CO)_6]$ with $[Cr(CO)_3(\eta\text{-}C_{16}H_{16})]$ to be intermediate between those for the corresponding reactions with free [2.2]paracyclophane and benzene. This is contrary to experimental observations, and the additional statistical preference for co-ordination of the $Cr(CO)_3$ unit to [2.2]paracyclophane or benzene rather than to $[Cr(CO)_3(\eta\text{-}C_{16}H_{16})]$ must also be considered. The partially metallated complex has only one arene face available for complexation, compared to two in both free [2.2]paracyclophane and benzene, which will further reduce the rate of reaction of $[Cr(CO)_6]$ with $[Cr(CO)_3(\eta\text{-}C_{16}H_{16})]$ by a factor of two. Accordingly, the preparation of $[\{Cr(CO)_3\}_2(\eta\text{-}C_{16}H_{16})]$ from $[Cr(CO)_3(\eta\text{-}C_{16}H_{16})]$ and hexacarbonylchromium occurs more slowly than the metallation of either *p*-xylene or [2.2]paracyclophane, and high temperatures are required to drive the reaction.[5] Furthermore, the yield of *ca.* <10% is low compared to complexation of the first $\{Cr(CO)_3\}$ unit, which takes place in near quantitative yields.

The larger cyclophane, [2.2.2]paracyclophane, shows similar trends to [2.2]paracyclophane. Scheme 2 shows that the repulsion between the rings in free [2.2.2]paracyclophane is of similar magnitude to that in [2.2]paracyclophane, but now it results from three interactions rather than two. The net repulsion per benzene ring is therefore reduced from 27 kJ mol^{-1} to 17 kJ mol^{-1}. Furthermore, the rings are no longer parallel and so van der Waals contacts between the hydrogen atoms may also contribute to the total repulsive energy, along with the familiar π–π repulsions. The hydrogen–hydrogen repulsions will remain approximately constant regardless of the degree of metallation, and so the differences in repulsion energies, and hence different reactivity of the complexes, will still be determined principally by changes in the π–π repulsions.

Complexation of one $\{Cr(CO)_3\}$ fragment reduces the π–π repulsions in [2.2.2]paracyclophane, but only by 10 kJ mol^{-1}, indicating that the reactivity should be enhanced relative to

---

† See Fig. 3 of ref. 6 for a detailed discussion of the methodology.

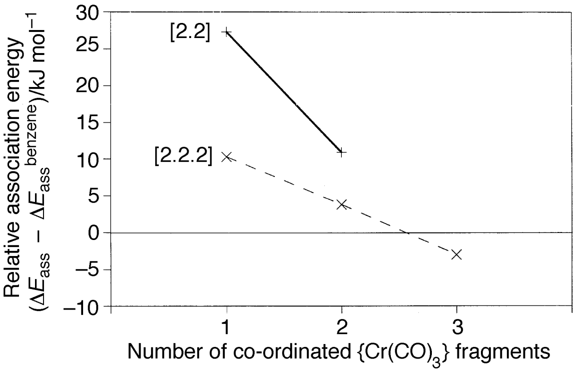

Fig. 3 Relative association energies ($\Delta E_{ass} - \Delta E_{ass}^{benzene}$/kJ mol^{-1}) for successive metallation of [2.2]- and [2.2.2]-paracyclophane

benzene, but not to the same extent as that observed in [2.2]paracyclophane. This conclusion is again contrary to the experimental rate constants, which suggest that [2.2.2]paracyclophane is more reactive than the [2.2] species. The reason for the discrepancy between calculation and experiment may again lie in the neglect of statistical factors in the former. [2.2.2]Paracyclophane has three available co-ordination sites, as opposed to only two in [2.2]paracyclophane, and consequently even in the absence of a thermodynamic preference for co-ordination to one or the other, we would anticipate a 1.5 fold enhancement of the rate constant in the former. We therefore conclude that a combination of both energetic and statistical factors is responsible for the high rate constant observed for the reaction of [Cr(CO)$_6$] with [2.2.2]paracyclophane.

In contrast to the first metallation, complexation of a second and third {Cr(CO)$_3$} fragment results in only very minor changes in π–π repulsions. Accordingly, the second and third arene faces behave essentially as isolated benzene rings, and the much reduced rates for the second and third metallations reflect this change. The high residual repulsive energy present even after three {Cr(CO)$_3$} units have been co-ordinated is probably largely due to H · · · H repulsions rather than π–π repulsions.

The relative stabilities of {Cr(CO)$_3$} complexes of both [2.2]paracyclophane and [2.2.2]paracyclophane are summarised in Fig. 3. The difference between the calculated association energy (ΔE_{ass}) and that on an isolated benzene ring ($\Delta E_{ass}^{benzene}$) is plotted as a function of the number of associated metal fragments. Several important conclusions emerge from this figure. First, the stabilities of the monometallated complexes of both [2.2]paracyclophane and [2.2.2]paracyclophane are significantly greater than the corresponding complex with benzene, due to the co-ordination-induced relief of π–π repulsions in the cyclophanes. In both cases, the addition of a single electron-withdrawing {Cr(CO)$_3$} fragment is sufficient to remove the majority of these π–π repulsions and further metallation is favoured over the reaction with benzene only to a minor extent. The contrast between first and second metallations is more marked in the [2.2]paracyclophane complexes, where the two arene rings lie parallel and close to each other and hence π–π repulsions are most significant. In the larger [2.2.2]paracyclophane system, where the distance between the centroids of the arene rings is much greater, π–π repulsions are in general less significant, and hence the relative stabilities of the complexes are less dependent on the degree of metallation.

Experimental

All reactions were carried out under an atmosphere of nitrogen gas using dried and degassed solvents. The Strohmeier reflux method[11] was used in all reactions in order to ensure that [Cr(CO)$_6$] was not lost from the reaction mixture by sublimation. The apparatus consisted of two reflux condensers connected in series, the lower one without cooling water, the upper one with cooling water. Any [Cr(CO)$_6$] which sublimes onto the lower condenser is then washed back into the reaction vessel by the solvent which condenses on the upper condenser. Hexacarbonylchromium was purchased from Aldrich Chemicals and was used without further purification, [2.2.2]paracyclophane ($C_{24}H_{24}$) was prepared according to the literature procedure.[12] Solution infrared spectra (1.0 cm^{-1} resolution) were recorded in a Specac solution cell (KBr windows, path length 0.1 mm) against a neat solvent background, using a dry-air purged Nicolet 750 FT spectrometer. Proton NMR spectra were recorded on a JEOL JNM-EX270 FTNMR spectrometer calibrated to internal SiMe$_4$.

Synthesis of [Cr(CO)$_3$(η-$C_{24}H_{24}$)] 1, [{Cr(CO)$_3$}$_2$(η-$C_{24}H_{24}$)] 2 and [{Cr(CO)$_3$}$_3$(η-$C_{24}H_{24}$)] 3

In a typical reaction, $C_{24}H_{24}$ (0.5 g, 1.6 mmol) and [Cr(CO)$_6$] (0.35 g, 1.6 mmol for **1**, 0.71 g, 3.2 mmol for **2** and 1.05 g, 4.8 mmol for **3**) were dissolved in 1,4-dioxane. The reaction mixture was heated to reflux for 36 h for **1**, 72 h for **2** and 120 h for **3**. The solvent was removed *in vacuo* and the yellow solid redissolved in CH_2Cl_2–hexane (1 : 1, v/v). Single crystals of **1** were obtained after storing the solution at 4 °C for 24 h and single crystals of **2** were obtained from slow evaporation of the solvent over several days. Crystals of **3** were obtained, but these were not suitable for single-crystal X-ray diffraction analysis. All compounds were obtained in yields exceeding 90% prior to recrystallisation.

Spectroscopic data for compound **1**: IR (KBr) 1966s, 1857s cm^{-1}; ^{1}H NMR (CDCl$_3$), δ 6.85 (d, J = 6.3, 4 H), 6.7 (d, J = 6.3, 4 H), 4.9 (s, 4 H), 3.1 (s, 4 H), 2.88 (d, J = 6.7, 4 H), 2.68 (d, J = 6.7 Hz, 4 H) [Found (Calc.): C, 72.3 (72.3); H, 5.4 (5.4)%].

Spectroscopic data for compound **2**: IR (KBr) 1958s, 1857s cm^{-1}; ^{1}H NMR (CDCl$_3$), δ 6.90 (s, 4 H), 5.00 (d, J = 6.9, 4 H), 4.90 (d, J = 6.9, 4 H), 2.96 (d, J = 6.6, 4 H), 2.93 (d, J = 6.6 Hz, 4 H), 2.60 (s, 4 H) [Found (Calc.): C, 61.0 (61.6); H, 3.85 (4.1)%].

Spectroscopic data for compound **3**: IR (KBr) 1951s, 1882s cm^{-1}; ^{1}H NMR (CDCl$_3$), δ 3.67 (s, 12 H), 2.18 (s, 12 H).

The spectroscopic data for all the compounds are in good agreement with those previously reported.[10]

Kinetic studies

Compounds [Cr(CO)$_6$] (80 mg, 0.36 mmol), $C_{24}H_{24}$ (113 mg, 0.36 mmol) and 1,4-dioxane (50 cm^3) were heated to reflux (solvent temperature ≈ 380 K). Aliquots (0.1 cm^3) were periodically withdrawn from the reaction mixture and the infrared spectrum of the aliquot recorded immediately after sampling. On completion of the reaction the solvent was removed under reduced pressure and the product was used for the next kinetics measurements in the manner outlined above.

The rate of reaction of [Cr(CO)$_6$] with the arenes was determined by monitoring the disappearance of ν(CO) from [Cr(CO)$_6$] at 1980 cm^{-1} (t_{1u}) with time. The concentration of [Cr(CO)$_6$] was determined from the absorbance at the analytical wavenumber, given that Beer's law holds over the concentration range used. Plots of ln(A_t/A_0) *versus* time (where A_t = absorbance at time t and A_0 = initial absorbance) gave first-order rate constants. Reagent concentrations were not corrected to account for the loss of material contained in each sampled aliquot.

Structural characterisation

Crystal diffraction data were collected on a Nicolet R3mV automated four-circle diffractometer equipped with Mo-Kα radiation (λ = 0.710 73 Å). Important crystallographic parameters are summarised in Table 3. The structures were solved by direct methods and developed by using alternating cycles of least-squares refinement on F and Fourier-difference synthesis. The non-hydrogen atoms were refined anisotropically while

Table 3 Crystallographic parameters for compounds **1** and **2**

	1	**2**
Formula	$C_{27}H_{24}CrO_3$	$C_{30}H_{24}Cr_2O_6$
T/K	293	293
Crystal system	Monoclinic	Monoclinic
Space group	$P2_1/n$	$P2_1/n$
a/Å	6.246(1)	9.878(3)
b/Å	14.436(3)	22.952(4)
c/Å	24.120(5)	12.429(4)
β/°	97.55(3)	112.33(2)
U/Å^3	2156(1)	2606(1)
Z	4	4
F(000)	936	1200
D_c/g cm^{-3}	1.38	1.49
μ/cm^{-1}	5.6	8.7
Crystal size/mm	0.25 × 0.15 × 0.10	0.78 × 0.45 × 0.15
θ range/°	2.5–27.5	2.5–25
h,k,l Index ranges	0–8, 0–18, −29 to 28	0–11, 0–27, −14 to 13
Data measured	5373	4692
Unique data	4756	4427
No. unique data with $[I \geqslant 2\sigma(I)]$	2176	3276
No. parameters	280	343
R^a	0.0455	0.0930
R'^b	0.0479	0.2776
Weighting scheme	$w^{-1} = \sigma^2(F) + 0.0009F^2$	$w^{-1} = \sigma^2(F) + 0.014F^2$
Largest shift/e.s.d.	0.002	0.001
Largest peak/e Å^{-3}	0.40	1.7

Empirical absorption corrections using the ψ-scan method. [a] $R = \Sigma[|F_o| - |F_c|]/\Sigma|F_o|$. [b] $R = \Sigma w^{\frac{1}{2}}[|F_o| - |F_c|]/\Sigma w^{\frac{1}{2}}|F_o|$.

hydrogens were placed in idealised positions [C−H 0.96 Å] and assigned a common isotropic thermal parameter (U = 0.08 Å^2). Structure solution and refinement used the SHELXTL PLUS program.[13]

Atomic coordinates, thermal parameters, and bond lengths and angles have been deposited at the Cambridge Crystallographic Data Centre (CCDC). See Instructions for Authors, *J. Chem. Soc., Dalton Trans.*, 1997, Issue 1. Any request to the CCDC for this material should quote the full literature citation and the reference number 186/424.

Computational details

Molecular orbital calculations. All calculations were based on approximate density functional theory using the Amsterdam Density Functional (ADF) package developed by Baerends and co-workers.[14] The local density approximation was employed using the parameterisation of Vosko *et al.*[15] for the exchange-correlation potential. Gradient corrections to exchange (Becke[16]) and correlation (Perdew[17]) functionals were included at each iteration of the self-consistent field procedure. The valence orbitals of Cr (3d, 4s and 4p) were represented by a triple-ζ Slater type orbital (STO) basis set. A double-ζ basis was employed for the 2s and 2p orbitals of C and O and the 1s orbital of H. For C and O this basis was augmented by a single 3d function, while for hydrogen a 2p orbital was used for polarisation. All electrons in lower shells were considered as core and treated according to the frozen-core approximation of Baerends *et al.*[18] An auxiliary set of s, p, d, f and g STO functions, centred on all nuclei, was used to fit the molecular density. Idealised model geometries were based on the experimental structures of $[Cr(CO)_3(\eta\text{-}C_{16}H_{16})]$ and $[Cr(CO)_3(\eta\text{-}C_{24}H_{24})]$. Within the $\{Cr(CO)_3\}$ fragments, the following bond lengths and angles were utilised: Cr−C 1.73, C−O 1.16 Å, O−C−Cr 180.0, C−Cr−C 90.0° and the chromium atom was placed 1.84 Å from the centroid of the co-ordinated ring. The centroids of the benzene rings were placed 3.02 Å and 4.36 Å apart to model [2.2]- and [2.2.2]-paracyclophane respectively.

Acknowledgements

P. J. D. acknowledges the Royal Society for a University Research Fellowship, D. G. H. thanks the Ramsay Memorial Fellowship Trust for a British Ramsay Fellowship and P. S. thanks the EPSRC for financial support.

References

1 J. Schulz and F. Vögtle, *Top. Curr. Chem.*, 1994, **172**, 41.
2 E. D. Laganis, R. H. Voegeli, R. T. Swann, R. G. Finke, H. Hopf and V. Boekelheide, *Organometallics*, 1982, **11**, 1415.
3 D. J. Cram and H. Steinberg, *J. Am. Chem. Soc.*, 1951, **73**, 5691; D. J. Cram and J. M. Cram, *Acc. Chem. Res.*, 1971, **4**, 204.
4 Y. Kai, N. Yasuoka and N. Kasai, *Acta Crystallogr., Sect. B*, 1978, **34**, 2840.
5 H. Ohno, H. Horita, T. Otsubo, Y. Sakata and S. Misumi, *Tetrahedron Lett.*, 1977, 265.
6 P. J. Dyson, D. G. Humphrey, J. E. McGrady, D. M. P. Mingos and D. J. Wilson, *J. Chem. Soc., Dalton Trans.*, 1995, 4039.
7 M. Vemura, *Adv. Met. Org. Chem.*, 1991, **2**, 195.
8 E. O. Fischer, K. Ofele, H. Essler, W. Frohlich, J. P. Mortensen and W. Semmlinger, *Chem. Ber.*, 1958, **91**, 2763.
9 D. A. Brown, N. J. Gogan and H. Sloan, *J. Chem. Soc.*, 1965, 6873.
10 C. Elschenbroich, J. Schneider, M. Wünsch, J.-L. Pierre, P. Baret and P. Chautemps, *Chem. Ber.*, 1988, **121**, 177.
11 W. Strohmeier, *Chem. Ber.*, 1961, **94**, 2490.
12 I. Tabushi, H. Yamada, Z. Yoshida and R. Oda, *Tetrahedron*, 1971, **27**, 4845.
13 G. M. Sheldrick, SHELXTL PLUS, Program package for structure solution and refinement, version 4.2, Siemens Analytical X-Ray Instruments, Madison, WI, 1990.
14 P. M. Boerrigter, G. te Velde and E. J. Baerends, *Int. J. Quantum Chem., Quantum Chem. Symp.*, 1988, **33**, 307.
15 S. H. Vosko, L. Wilk and M. Nusair, *Can. J. Phys.*, 1980, **58**, 1200.
16 A. D. Becke, *Phys. Rev. A*, 1988, **38**, 3098.
17 J. P. Perdew, *Phys. Rev. B*, 1986, **33**, 8822.
18 E. J. Baerends, D. E. Ellis and P. Ros, *Chem. Phys.*, 1973, **2**, 41.

Received 20*th January* 1997; *Paper* 7/00484B